J. Fluid Mech. (1969), *vol.* 36, *part* 4, *pp.* 805–829
Printed in Great Britain

On some problems of similarity flow of fluid with a free surface

By Z. N. DOBROVOL'SKAYA
Computing Centre of the Academy of Sciences of the USSR, Moscow

(Received 6 May 1968)

The paper presents the method of solving a class of two-dimensional problems of the similarity flow of an incompressible fluid with a free surface. The fluid is assumed to be non-viscous and weightless. We consider two-dimensional irrotational similarity flows with dimensionless hydrodynamic characteristics depending only on the ratios x/v_0t, y/v_0t, where x, y are Cartesian co-ordinates, t is time and v_0 is a constant of the velocity dimension.

The proposed method is based upon using the function introduced by Wagner (1932) and can be applied to the problems where the flow region is bounded by free surfaces and uniformly moving (or fixed) rectilinear impermeable boundaries. Introduction of Wagner's function makes it possible to reduce each of the problems under consideration to a non-linear singular integral equation for the real function.

The method is illustrated by solving the classical problem of the uniform symmetrical entry of a wedge into a half-plane of a fluid.

1. Introduction

Hydrodynamic problems of flow with free surfaces (in particular, the water-entry problems) are essentially non-linear. The difficulty in solving these problems is that of satisfying the non-linear boundary conditions on the free surface, which is not a stream-surface in unsteady motion.

The problems under consideration have been studied by many authors. The theoretical analysis of similarity flows of an incompressible fluid was first presented by Wagner (1932) who obtained, in particular, an approximate solution of the wedge water-entry problem.

Thereafter this problem was investigated by Pierson (1950), Garabedian (1953), Borg (1957), Moiseev *et al.* (1959) and others. The similar problem of the impact of a water wedge on a plate was studied by Cumberbatch (1960). But until now no exact solutions (analytical or numerical) of these problems have been obtained.

The complete solution was obtained only for the linearized wedge water-entry problem. For the case of a compressible fluid it was given by Grigoryan (1956) and Sagomonyan (1956); the results for an incompressible fluid were first written explicitly by Mackie (1962).

In § 2 of the present paper the definition of Wagner's function and its main

properties are recalled. In § 3 we give the method of Wagner's function for reducing the problems under examination to a singular integral equation. In § 4 the integral equation is derived for the problem of the uniform symmetrical entry of a wedge into a half-plane of a fluid. In § 5 we show the applicability of the successive-iterations method for solving the integral equation obtained and give the scheme of numerical integration of this equation.

Results of the numerical solution of the wedge problem are given in § 6. Presented and analyzed here are the free surfaces for different wedge angles and the curves of the pressure distribution along the wedge; in particular, the free-surface behaviour near the wedge is investigated. The obtained numerical solution is compared with the analytical solution of the linearized problem.

2. Wagner's function

Let x, y be fixed Cartesian co-ordinates in the plane of flow (which we shall call the 'physical plane'), t, time and $\xi = x/(v_0 t)$, $\eta = y/(v_0 t)$, the dimensionless similarity variables ($v_0 = \text{const.}$). In the (ξ, η)-plane a stationary region corresponds to the physical flow region varying with time. But the part of the boundary of the flow region, corresponding to the free surface, is unknown in advance in both planes.

The velocity potential $\phi(x, y, t)$ and the stream-function $\psi(x, y, t)$ of the flows under consideration have the form

$$\phi(x, y, t) = v_0^2 t \Phi(\xi, \eta), \quad \psi(x, y, t) = v_0^2 t \Psi(\xi, \eta),$$

where $\Phi(\xi, \eta)$ and $\Psi(\xi, \eta)$ are harmonic functions of ξ and η.

$$U(z, t) = \phi(x, y, t) + i\psi(x, y, t)$$

is the complex velocity potential in the z-plane ($z = x + iy$). Let us introduce function

$$V(\zeta) = \Phi(\xi, \eta) + i\Psi(\xi, \eta) \quad (\zeta = \xi + i\eta).$$

The function $V'(\zeta)$ is connected to the complex velocity $U'_z(z, t)$ by the obvious relation

$$U'_z(z, t) = v_0 V'(\zeta). \tag{2.1}$$

Therefore, it is natural to call the function $V'(\zeta)$ the complex velocity and $V(\zeta)$ the complex velocity potential in the ζ-plane.

Wagner's function h can be determined as follows†

$$h(\zeta) = \int_{\infty}^{\zeta} \sqrt{\left(\frac{dV'(\zeta)}{d\zeta}\right)} \, d\zeta. \tag{2.2}$$

The purpose of introducing Wagner's function is that, in the plane of this function, the free surface of a fluid is always represented by a segment of a straight

† Wagner introduced the function h (for the wedge water-entry problem) in a slightly different way, namely

$$h = \int^{z} \sqrt{\left(\frac{dU'_z(z, t)}{dz}\right)} \, dz,$$

where $z = x + iy$ and x, y are the Cartesian co-ordinates moving uniformly with the wedge.

line (or by a broken line). We shall demonstrate below that for the flows under consideration the flow region bounded by the free surfaces and the uniformly moving (or fixed) rectilinear impermeable boundaries, is always known in the plane of Wagner's function. For this purpose we represent the integrand expression of formula (2.2) in the form

$$\sqrt{\left(\frac{dV'(\zeta)}{d\zeta}\right)}\,d\zeta = \sqrt{(dV'(\zeta)\,d\zeta)} \tag{2.3}$$

and investigate first of all the behaviour of function (2.3) on the free surface, following Wagner's presentation.

In the similarity flow with the variables

$$\xi = \frac{x}{v_0 t}, \quad \eta = \frac{y}{v_0 t} \tag{2.4}$$

the following relation holds for the velocity vector $\mathfrak{U}(x, y, t)$

$$\mathfrak{U}(x, y, t) = v_0 \mathfrak{V}\left(\frac{x}{v_0 t}, \frac{y}{v_0 t}\right). \tag{2.5}$$

After differentiating the left- and right-hand sides of (2.5) with respect to t, we obtain

$$\frac{d\mathfrak{U}(x, y, t)}{dt} = -v_0\left[\frac{\partial \mathfrak{V}(x/v_0 t, y/v_0 t)}{\partial(x/v_0 t)}\frac{x}{v_0 t^2} + \frac{\partial \mathfrak{V}(x/v_0 t, y/v_0 t)}{\partial(y/v_0 t)}\frac{y}{v_0 t^2}\right]. \tag{2.6}$$

Let us consider (2.6) on the free surface when t is fixed. With t fixed, the variables x, y on the free surface are single-valued functions of the arc length s measured along the free surface. In this case (2.6) reduces to the form

$$\frac{d\mathfrak{U}(x, y, t)}{dt} = -\frac{\partial \mathfrak{U}(x, y, t)}{\partial s}\left(\frac{ds}{dx}\frac{x}{t} + \frac{ds}{dy}\frac{y}{t}\right). \tag{2.7}$$

The expression in the brackets in (2.7) is a scalar function, and hence the vector $\partial \mathfrak{U}(x, y, t)/\partial s$ has the same direction as the acceleration vector $d\mathfrak{U}(x, y, t)/dt$ at any point of the free surface. Pressure on the free surface being constant, the pressure gradient on the free surface is normal to the latter at any of its points. Therefore, according to the Euler equations, the acceleration $d\mathfrak{U}/dt$ of fluid particles lying on the free surface is also normal to the free surface. Taking this into account, it follows from (2.7) that the increment of the velocity vector along the free-surface element is normal to the free surface at any of its points.

The same fundamental fact can be re-proved in a more formal way. In fact, the total differential of the function $\mathfrak{U}(x, y, t)$ has the form

$$d\mathfrak{U}(x, y, t) = \frac{\partial \mathfrak{U}(x, y, t)}{\partial t}\,dt + \frac{\partial \mathfrak{U}(x, y, t)}{\partial x}\,dx + \frac{\partial \mathfrak{U}(x, y, t)}{\partial y}\,dy. \tag{2.8}$$

Introducing the similarity variables (2.4) and taking into account (2.5), the relation (2.8) can be reduced without difficulty to the form

$$d\mathfrak{U}(x, y, t) = v_0\left[\frac{\partial \mathfrak{V}(\xi, \eta)}{d\xi}\,d\xi + \frac{\partial \mathfrak{V}(\xi, \eta)}{\partial \eta}\,d\eta\right] \tag{2.9}$$

or, as might be expected,

$$d\mathfrak{U}(x, y, t) = v_0 d\mathfrak{V}(\xi, \eta). \tag{2.10}$$

Formula (2.10) shows that in the flows under consideration the differential of function $\mathfrak{U}(x, y, t)$ with respect to variables x, y, t coincides (to within the constant factor v_0) with the differential of function $\mathfrak{V}(\xi, \eta)$ with respect to variables ξ, η. Let us fix variable t and consider (2.10) on the free surface. The vector $d\mathfrak{U}(x, y, t)$, having the same direction as the acceleration vector, is normal to the free surface. Then, according to (2.10) ,the direction of the normal to the free surface in the (ξ, η)-plane is also the direction of the vector $d\mathfrak{V}(\xi, \eta)$ which is the increment of the velocity vector along the free-surface element.†

This fact makes it possible to construct the free-surface image in the plane of Wagner's function.

Therefore, let ζ be a point of the free surface $\eta = \eta(\xi)$ and let the contour of integration in formula (2.2) include the part of the free surface from infinity‡ to ζ (the path of integration is chosen so that the flow region would be from the left). Now let us investigate the behaviour of the argument of function

$$\sqrt{(dV'(\zeta)\, d\zeta)}$$

on the free surface. As shown above, the increment $d\overline{V'(\zeta)}$ of the velocity vector along the free-surface element is normal to it and can be directed along the outward or inward normal.

Let us first consider the case when (under the chosen path of integration) the vector $d\overline{V'(\zeta)}$ is in the outward normal direction to the free surface. The argument of vector $d\zeta$ at a point M_1 on the free surface BC is denoted by θ (figure 1). Then $\arg d\overline{V'(\zeta)} = \theta - \frac{1}{2}\pi$ as $d\zeta$ and $d\overline{V'(\zeta)}$ are mutually orthogonal, and hence

$$\arg dV'(\zeta) = \tfrac{1}{2}\pi - \theta$$

as vectors $dV'(\zeta)$ and $d\overline{V'(\zeta)}$ are conjugate. Taking this into account, we obtain

$$\arg \sqrt{(dV'(\zeta)\, d\zeta)} = \tfrac{1}{2}[\arg dV'(\zeta) + \arg d\zeta] = \tfrac{1}{4}\pi. \tag{2.11}$$

Condition (2.11) is satisfied at any point of the free surface. Therefore the increment of Wagner's function $h(\zeta)$ has the argument $\frac{1}{4}\pi$ on the considered part of the free surface.

† The increment of the velocity vector is not orthogonal to the free surface in the case of flow with the similarity law of the form

$$\mathfrak{U}(x, y, t) = ct^{\gamma}\mathfrak{V}(\xi, \eta), \quad \text{where} \quad \xi = \frac{x}{ct^{\gamma+1}}, \quad \eta = \frac{y}{ct^{\gamma+1}}.$$

In this case the relations

$$\frac{d\mathfrak{U}(x, y, t)}{dt} = \frac{\gamma}{t}\mathfrak{U}(x, y, t) - (\gamma+1)\frac{\partial \mathfrak{U}(x, y, t)}{\partial S}\left(\frac{ds}{\partial x}\frac{x}{t} + \frac{ds}{dy}\frac{y}{t}\right),$$

$$d\mathfrak{U}(x, y, t) = \gamma c t^{\gamma-1}\, \mathfrak{V}(\xi, \eta)\, dt + ct^{\gamma}\, d\mathfrak{V}(\xi, \eta)$$

hold, instead of the conditions (2.7) and (2.10)

As will be seen from the following, the similarity of this form excludes the construction of the flow region in the plane of Wagner's function before solving the problem.

‡ In the similarity problems under consideration, the free surface reaches the point at infinity of the ζ-plane.

In a similar way it can be shown that the argument of increments of Wagner's function is equal to $-\frac{1}{4}\pi$ on those parts of the free surface where the vector $d\overline{V'(\zeta)}$ is in the inward normal direction to the free surface.†

Thus, the free-surface image in the plane of Wagner's function is in the general case a broken line, composed of the rectilinear segments inclined to the axis of abscissas at the angle $\frac{1}{4}\pi$ or $-\frac{1}{4}\pi$. If the vector $d\overline{V'(\zeta)}$ on the free surface does not change its direction from outward normal to the inward one (or conversely), then the free surface is represented in the plane of Wagner's function simply by a rectilinear segment making the angle $\frac{1}{4}\pi$ or $-\frac{1}{4}\pi$ with the axis of abscissas.

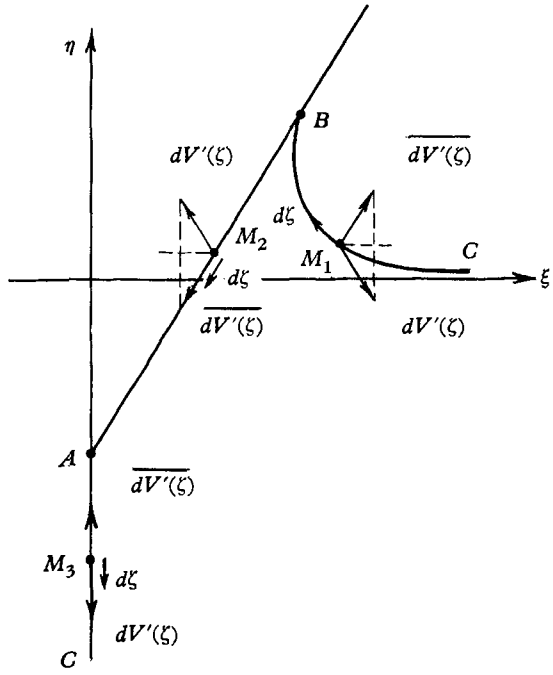

FIGURE 1. The directions of vectors $d\overline{V'(\zeta)}$ and $d\zeta$ on the free surface CB, and rectilinear impermeable boundaries BA and AC (illustration to the formula by Wagner (1932)).

We investigate now the behaviour of the function $h(\zeta)$ on the rectilinear segment AB (figure 1), being the image of a uniformly moving impermeable rectilinear boundary. According to the impermeability condition all the fluid particles on the impermeable contour have the same normal (to the boundary) velocity. Therefore, the velocity-vector increment $d\overline{V'(\zeta)}$ at a point M_2 on the impermeable rectilinear boundary is directed along the boundary, being in the same direction as the vector $d\zeta$, or opposite to the latter. In the first case $\arg d\overline{V'(\zeta)} = \arg d\zeta$ whence it follows that $\arg dV'(\zeta) = -\arg d\zeta$, and then the function $\sqrt{(dV'(\zeta)\,d\zeta)}$ has the argument equal to zero (or $\pm\pi n$) on the impermeable boundary. In the case when $d\zeta$ and $d\overline{V'(\zeta)}$ have opposite directions, it can easily be shown that

† In general, the argument of increments of function $h(\zeta)$ may differ from the indicated values $\pm\frac{1}{4}\pi$ by $2\pi n$, where the integer n is determined by the frame of reference and the flow kinematics on the whole.

$\arg \sqrt{(dV'(\zeta)\,d\zeta)} = \pm \frac{1}{2}\pi$ (or $\pm \frac{1}{2}\pi \pm \pi n$), the sign depending on the direction of path along the boundary.

If the impermeable boundary AC (figure 1) is stationary in the (x, y)-plane, the behaviour of the argument of function $\sqrt{(dV'(\zeta)\,d\zeta)}$ is the same as in the case just considered. Thus, the image of the uniformly moving or stationary rectilinear impermeable boundary in the plane of Wagner's function is a rectilinear segment parallel or orthogonal to the axis of abscissas.

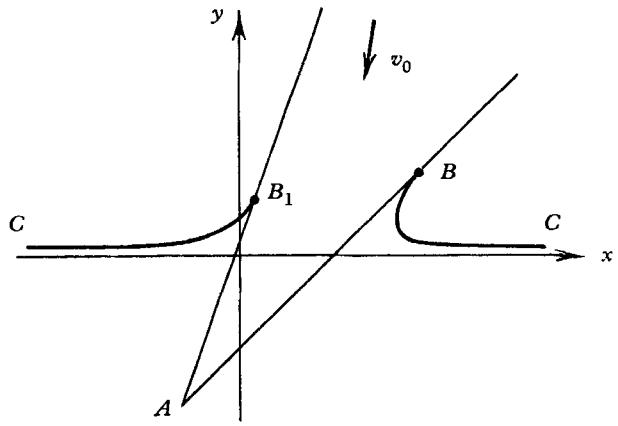

FIGURE 2. The flow region in the physical plane x, y for the unsymmetrical entry of a wedge into a fluid.

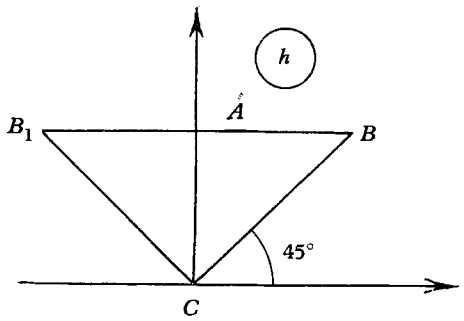

FIGURE 3. The flow region in the plane of Wagner's function for the symmetrical and unsymmetrical entry of a wedge into a fluid, and for the impact of a water wedge on a wall.

Below we consider only such problems in which the flow region is bounded by the free surfaces and uniformly moving (or stationary) impermeable rectilinear boundaries. For the problems of this class, as seen from the above, the flow region is always represented in the plane of Wagner's function by a polygon. For example, in the case of symmetrical solid-wedge entry into a half-plane of a fluid (or into a fluid wedge) the flow region is represented in the plane of Wagner's function by a rectangular isosceles triangle. In the case of unsymmetrical wedge entry the flow region in the plane of Wagner's function is of the same form as in the symmetrical case (figures 2 and 3).

The method of Wagner's function can be also applied to solve the problem

of the impact of a water wedge on a wall (figure 4), as in this case the flow region in the plane of Wagner's function is known and represented by the same triangle as in the wedge water-entry problem.

In the problem of the uniform spreading of a constant pressure wave over the free surface being initially non-perturbed, the flow region in the plane of Wagner's function is represented by a square.

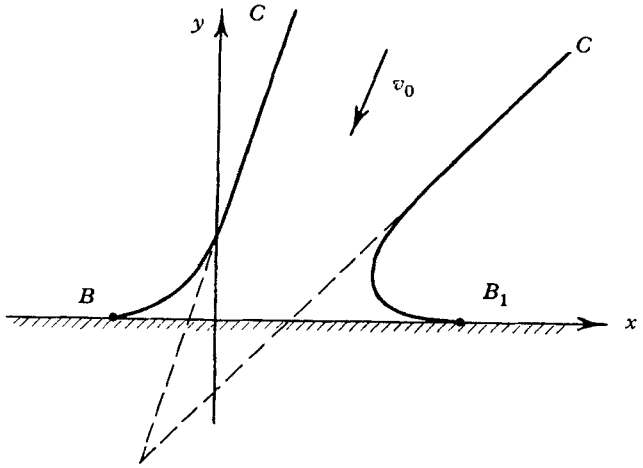

FIGURE 4. The flow region in the physical plane x, y for the impact of a water wedge on a wall.

3. Method of Wagner's function for reducing the problems under consideration to a non-linear singular integral equation

The essence of the method consists in the following. The problem of the similarity potential flow in the region bounded by the free surface and impermeable rectilinear boundaries can be formulated as the problem of determination, in the flow region (in the similarity (ξ, η)-plane), of the velocity potential $\Phi(\xi, \eta)$, a harmonic function, satisfying the constant-pressure condition and the kinematic condition on the free surface $\eta = \eta(\xi)$, and the impermeability conditions on the solid boundaries.

Let $V(\zeta) = \Phi(\xi, \eta) + i\Psi(\xi,\eta)$ be the complex velocity potential in the ζ-plane $(\zeta = \xi + i\eta)$. We introduce the auxiliary parametric variable $w = u + iv$ and consider the analytical function $\zeta = \zeta(w)$ mapping conformally the upper half-plane $\operatorname{Im} w > 0$ onto the flow region in the ζ-plane in such a way that the free surface of a fluid is represented by a segment L of the real axis of the w-plane and the rectilinear impermeable boundaries by the remaining part of the real axis which we denote by l (both L and l may contain a point at infinity).

Introduction of function $\zeta(w)$ makes it possible to reduce the problem to the determination of two analytical functions $V(w)$ and $\zeta(w)$ in the upper half-plane $\operatorname{Im} w > 0$ using the following boundary conditions: functions $V(u)$ and $\zeta(u)$ have to satisfy the constant pressure and kinematic conditions on segment L, and the impermeability and obvious geometric conditions on l; the latter follows from

the fact that the argument of the function $\zeta'(u)$ on l is known and equal to the constant or piecewise constant function. Thus, both on L and l there are two conditions for the determination of two functions $V(w)$ and $\zeta(w)$ analytical in the upper half-plane.

Let us introduce Wagner's function $h(\zeta)$. In the plane of this function the flow region is represented by a polygon. By means of the Schwarz–Christoffel formula we can write the function $h = h(w)$ which maps conformally the upper half-plane $\operatorname{Im} w > 0$ onto the interior of the polygon in the h-plane. Elimination of the variable h from the expression $h = h(w)$ and relation (2.2) gives an explicit expression for the complex velocity $V'(w)$ in terms of the mapping function $\zeta(w)$. The expression of function $V'(w)$ in terms of $\zeta(w)$ gives a possibility of excluding an unknown function $V(w)$ from the obtained boundary-value problem for two functions $V(w)$ and $\zeta(w)$, and the problem is thus reduced to the determination of function $\zeta(w)$, analytical in the upper half-plane $\operatorname{Im} w > 0$, which has to satisfy the kinematic condition on segment L and the geometric condition on l. The second condition on each of these intervals (the constant-pressure condition on L and the impermeability condition on l) has already been used for the determination of the flow region in the plane of Wagner's function.

Introduce the real function $f(u)\,(u \in L)$ representing the argument of $\zeta'(u)$ on L. Then, remembering that the argument of function $\zeta'(u)$ on l is known, we can write (by means of the Schwarz integral) the representation of the mapping function $\zeta(w)$ in terms of the real function $f(u)$. The substitution of $\zeta(w)$ expressed in terms of $f(u)$ into the kinematic condition on the interval L gives a non-linear singular integral equation for the determination of $f(u)$. Function $f(u)$ being determined, the hydrodynamic problem can be considered as solved since the mapping function $\zeta(w)$ and the complex velocity $V'(w)$ at any point of the flow region are expressed in terms of the function $f(u)$ by quadratures.

4. Symmetrical entry of a wedge

We consider uniform symmetrical entry of a wedge into a half-plane of a fluid which is assumed to be incompressible, non-viscous and weightless, the wedge angle $2\alpha_0$ being arbitrary ($\alpha_0 < \frac{1}{2}\pi$).

Let x, y be Cartesian co-ordinates with the origin at the point of intersection of the unperturbed free surface with the axis of symmetry (the y-axis is directed opposite to the wedge movement along the axis of symmetry). Because of the symmetry only the half $x \geqslant 0$ of the flow region is considered.

As the flow under consideration is the similarity flow, the velocity potential $\phi(x, y, t)$ has the form

$$\phi(x, y, t) = v_0^2 t \Phi(\xi, \eta), \tag{4.1}$$

where $\xi = x/v_0 t$, $\eta = y/v_0 t$ (v_0 being the velocity of the wedge), and $\Phi(\xi, \eta)$ is a harmonic function of ξ and η in the flow region $CBAC$ (figure 5). On the boundary of the flow region, the function $\Phi(\xi, \eta)$ has to satisfy the following conditions: on the free surface $\eta = \eta(\xi)$, the constant pressure condition

$$\Phi(\xi,\eta) - \xi \frac{\partial \Phi}{\partial \xi} - \eta(\xi) \frac{\partial \Phi}{\partial \eta} + \frac{1}{2}\left(\frac{\partial \Phi}{\partial \xi}\right)^2 + \frac{1}{2}\left(\frac{\partial \Phi}{\partial \eta}\right)^2 = 0 \tag{4.2}$$

and the kinematic condition

$$\frac{\partial\Phi}{\partial\eta}-\eta'(\xi)\frac{\partial\Phi}{\partial\xi}+\xi\eta'(\xi)-\eta(\xi)=0; \tag{4.3}$$

on the wedge and axis of symmetry, the impermeability conditions

$$\frac{\partial\Phi}{\partial\xi}\cos\alpha_0-\frac{\partial\Phi}{\partial\eta}\sin\alpha_0=\sin\alpha_0 \quad \text{on} \quad AB, \tag{4.4}$$

$$\frac{\partial\Phi}{\partial\xi}=0 \quad \text{on} \quad AC. \tag{4.5}$$

The free surface at infinity has to approach the unperturbed free surface asymptotically.

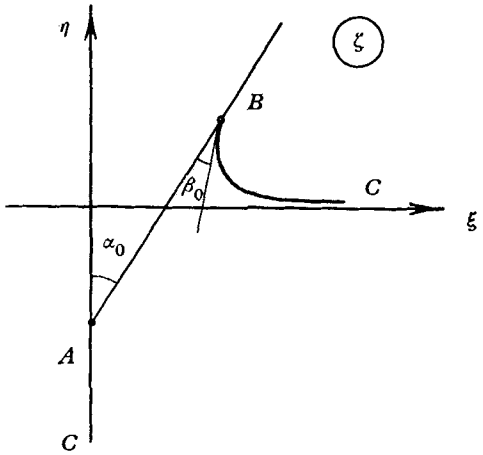

FIGURE 5. The half of the flow region $CBAC$ in the similarity plane $\zeta=\xi+i\eta$ for the symmetrical entry of a wedge into a fluid.

The wedge-entry problem can be reduced, first, to the boundary-value problem for two functions analytical in the upper half-plane. Therefore, let

$$V(\zeta)=\Phi(\xi,\eta)+i\Psi(\xi,\eta)$$

be the complex velocity potential in the ζ-plane ($\zeta=\xi+i\eta$). We introduce $w=u+iv$ and consider an analytical function $\zeta=\zeta(w)$ which maps conformally the upper half-plane $\operatorname{Im} w>0$ onto the flow region in the ζ-plane in such a way that the points $\zeta=\zeta_B$ (point of contact), $\zeta_A=-i$ (wedge apex) and $\zeta=\infty$ correspond to $w=0$, $w=1$ and $w=\infty$ respectively (figure 6). In so doing the free surface of a fluid will be represented by the real negative semi-axis of the w-plane.

Conditions (4.2) and (4.3) take the form

$$\zeta'(u)\overline{\zeta'(u)}\operatorname{Re}V(u)-\operatorname{Re}[\zeta(u)\overline{\zeta'(u)}\,V'(u)]+\tfrac{1}{2}V'(u)\,\overline{V'(u)}=0 \quad (-\infty<u\leqslant 0), \tag{4.6}$$

$$\operatorname{Re}[iV'(u)]=\operatorname{Re}[i\zeta'(u)\overline{\zeta(u)}] \quad (-\infty<u\leqslant 0). \tag{4.7}$$

On segment $0\leqslant u\leqslant 1$ two conditions have to be satisfied: condition (4.4) which can be reduced to the form

$$\operatorname{Re}[iV'(u)]=|\zeta'(u)|\sin\alpha_0 \quad (0\leqslant u\leqslant 1), \tag{4.8}$$

and the obvious geometrical condition

$$\arg \zeta'(u) = -(\tfrac{1}{2}\pi + \alpha_0) \quad (0 \leqslant u \leqslant 1). \tag{4.9}$$

When $u \geqslant 1$, we have condition (4.5) taking the form

$$\operatorname{Re}[iV'(u)] = 0 \quad (1 \leqslant u \leqslant \infty), \tag{4.10}$$

and geometrical condition

$$\arg \zeta'(u) = -\tfrac{1}{2}\pi \quad (1 \leqslant u < \infty). \tag{4.11}$$

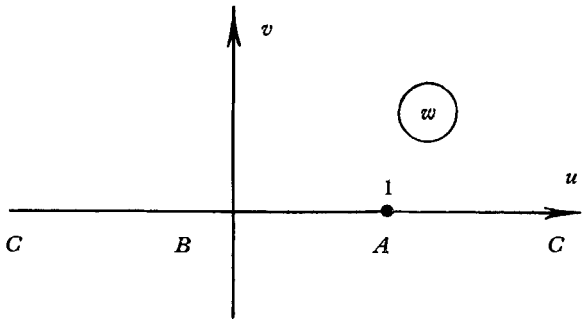

FIGURE 6. The image of the flow region $CBAC$ in the w-plane for the symmetrical entry of a wedge.

The problem is thus reduced to the determination of two functions $V(w)$ and $\zeta(w)$, analytical in the upper half-plane, satisfying boundary conditions (4.6)–(4.11) on the real axis.

We reduce the obtained boundary-value problem to the determination of the function $\zeta(w)$. To this end, we introduce Wagner's function

$$h(\zeta) = \int_{\infty}^{\zeta} \sqrt{\left(\frac{dV'(\zeta)}{d\zeta}\right)}\, d\zeta. \tag{4.12}$$

In the plane of this function the flow region $CBAC$ is represented by the interior of the isosceles right triangle (with the size unknown in advance) depicted in figure 7. The function $h(w)$, conformally mapping the upper half-plane onto the interior of the triangle in the h-plane with the correspondence of the angular points indicated in figures 6 and 7, has the form

$$h = ic_0 \int_{\infty}^{w} w^{-\frac{3}{4}}(w-1)^{-\frac{1}{2}}\, dw \quad (\operatorname{Im} c_0 = 0). \tag{4.13}$$

Eliminating the variable h from expressions (4.12) and (4.13) and taking into account that $V'(\zeta_B) = \bar{\zeta}_B$ (see Dobrovol'skaya 1965), we obtain

$$V'(w) = \bar{\zeta}_B \zeta'(w) - c_0^2 \zeta'(w) \int_0^w w^{-\frac{3}{2}}(w-1)^{-1} \frac{1}{\zeta'(w)}\, dw. \tag{4.14}$$

Formula (4.14) gives an explicit representation of the complex velocity in terms of the derivative of the function $\zeta(w)$ everywhere in the upper half-plane $\operatorname{Im} w > 0$. It should be noted that representation (4.14), obtained with the help of Wagner's function, is the consequence of conditions (4.6), (4.8) and (4.10)

since these conditions have been used for the determination of the flow region in the plane of Wagner's function. Eliminating function $V'(u)$ from the kinematic condition (4.7) with the help of (4.14), we obtain the following boundary condition for function $\zeta(u)$ on the real negative semi-axis $u \leqslant 0$

$$\mathrm{Re}\left\{i\zeta'(u)\int_0^u \left[\overline{\zeta'(u)} + c_0^2 u^{-\frac{3}{2}}(u-1)^{-1}\frac{1}{\zeta'(u)}\right] du\right\} = 0. \tag{4.15}$$

On the positive semi-axis, the function $\zeta(u)$ has to satisfy condition (4.9) for $0 \leqslant u \leqslant 1$ and (4.11) for $1 \leqslant u < +\infty$.

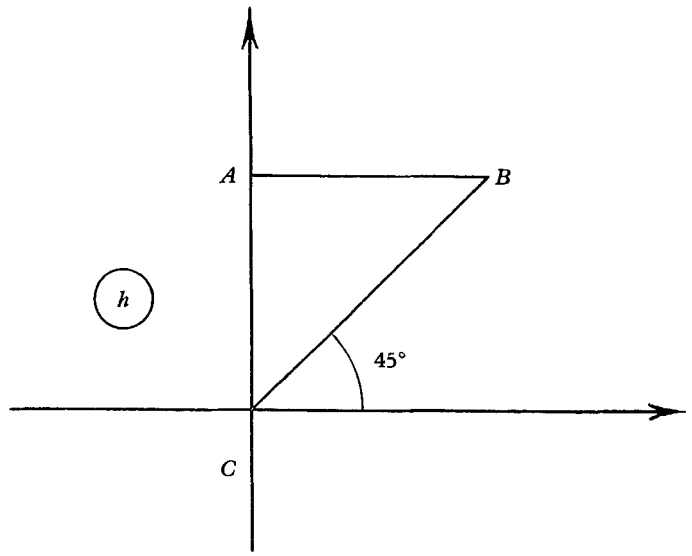

FIGURE 7. The flow region $CBAC$ in the plane of Wagner's function for the symmetrical entry of a wedge.

The problem is thus reduced to the determination of the function $\zeta(w)$, analytical in the upper half-plane $\mathrm{Im}\, w > 0$ from the boundary conditions (4.15), (4.9) and (4.11) on the real axis.

The boundary-value problem for $\zeta(w)$ will be reduced below to the integral equation for a real function $f(u)$ connected with $\zeta'(u)$, when $-\infty < u \leqslant 0$, by the relation

$$\arg \zeta'(u) = -\pi[f(u)+1] \quad (-\infty < u \leqslant 0). \tag{4.16}$$

The function $f(u)$ has to satisfy the condition

$$f(u) \to 0 \quad \text{when} \quad u \to -\infty, \tag{4.17}$$

as the free surface has to approach asymptotically the unperturbed free surface at long distances from the wedge. Using (4.16) and taking into account that the argument of function $\zeta'(u)$ for $0 \leqslant u < +\infty$ is known from the boundary conditions (4.9) and (4.11), we can write (with the help of the Schwarz integral for the upper half-plane) the representation of mapping function $\zeta(w)$ in terms of the real function $f(u)$. This representation has the form

$$\zeta'(w) = -icw^{-\frac{1}{2}+\alpha}(w-1)^{-\alpha}\exp\left[-\int_{-\infty}^{0}\frac{f(u)}{u-w}du\right] \quad (c > 0,\ \alpha = \alpha_0/\pi). \tag{4.18}$$

Using the Sokhotsky–Plemelj formula for the limit values of the Cauchy-type integral of expression (4.18), we can write the limit values of $\zeta'(w)$ (determined by (4.18)) when variable w tends to the real value u from the upper half-plane $\operatorname{Im} w > 0$. The substitution of $\zeta'(u)$ expressed in terms of $f(u)$ into the kinematic condition (4.15) gives the following non-linear singular integral equation for the determination of the function $f(u)$†

$$f(u) = -\frac{1}{\pi}\frac{c_0^2}{c^2}\int_{-\infty}^{u} \frac{u^{-1-\alpha}(u-1)^{-1+\alpha}\exp\left[\int_{-\infty}^{0}\frac{f(u_1)}{u_1-u}\,du_1\right]}{\int_0^u iu^{-\frac{1}{2}+\alpha}(u-1)^{-\alpha}\exp\left[-\int_{-\infty}^{0}\frac{f(u_1)}{u_1-u}\,du_1\right]du}\,du. \tag{4.19}$$

It is seen from (4.14), (4.18) and (4.19) that the solution of the problem contains two real parameters (c and c_0) and a complex parameter ζ_B; the real and imaginary parts of the latter are connected to each other by the obvious dependence

$$\xi_B = (1+\eta_B)\operatorname{tg}\alpha_0. \tag{4.20}$$

Thus, the solution contains real parameters c, c_0 and η_B for which determination there are three conditions:

$$\zeta(1) = -i, \tag{4.21}$$

$$\operatorname{Im}\zeta(u) \to 0 \quad \text{when} \quad u \to -\infty, \tag{4.22}$$

$$V'(\zeta) = i \quad \text{at} \quad \zeta = -i. \tag{4.23}$$

Using these conditions, we find that the value c_0^2/c^2 from integral equation (4.19) is determined by the following functional

$$\frac{c_0^2}{c^2} = \frac{\int_0^1 u^{-\frac{1}{2}+\alpha}(1-u)^{-\alpha}\exp\left[-\int_{-\infty}^{0}\frac{f(u_1)}{u_1-u}\,du_1\right]du}{\int_0^1 u^{-1-\alpha}(1-u)^{-1+\alpha}\exp\left[\int_{-\infty}^{0}\frac{f(u_1)}{u_1-u}\,du_1\right]du}. \tag{4.24}$$

For the numerical integration of (4.19), it is more convenient to introduce positive variables of integration $t = (1-u)^{-1}$ and $\tau = (1-u_1)^{-1}$ which vary within $0 \leqslant t \leqslant 1$ and $0 \leqslant \tau \leqslant 1$. Then, (4.19) is transformed to

$$f(t) = \frac{1}{\pi}\frac{c_0^2}{c^2}\int_0^t \frac{(1-t)^{-1-\alpha}\exp\left[t\int_0^1\frac{f(\tau)}{\tau(\tau-t)}\,d\tau\right]}{\int_t^1 t^{-\frac{3}{2}}(1-t)^{-\frac{1}{2}+\alpha}\exp\left[-t\int_0^1\frac{f(\tau)}{\tau(\tau-t)}\,d\tau\right]dt}\,dt \equiv \frac{1}{\pi}\frac{c_0^2}{c^2}I(t) \tag{4.25}$$

(the notation $I(t)$ is introduced for brevity of the subsequent discussion). Introducing variable $r = (1+u)^{-1}$ into expression (4.24), we obtain

$$\frac{c_0^2}{c^2} = \frac{\int_{\frac{1}{2}}^1 r^{-\frac{3}{2}}(1-r)^{-\frac{1}{2}+\alpha}(2r-1)^{-\alpha}\exp\left\{-\int_0^1\frac{f(\tau)\,d\tau}{\tau[\tau\{2-(1/r)\}-1]}\right\}dr}{\int_{\frac{1}{2}}^1 (1-r)^{-1-\alpha}(2r-1)^{-1-\alpha}\exp\left\{\int_0^1\frac{f(\tau)\,d\tau}{\tau[\tau\{2-(1/r)\}-1]}\right\}dr}. \tag{4.26}$$

† A copy of the author's derivation of this equation, which is taken from Dobrovol'skaya (1965), will be sent to any interested reader on request to the Editor.

Thus, the wedge water-entry problem has been reduced to the determination of the solution of the non-linear singular integral equation (4.25) for the real function $f(t)$.

The function $f(t)$ at any point $t \in [0, 1]$ is, by definition (to within the constant factor and sum), the angle of inclination of the free surface to the ξ-axis at the corresponding point of the free surface, and because of this, $f(t)$ is bounded on the whole segment $[0, 1]$ including its ends ($t = 1$ corresponds to the point of contact of the free surface with the wedge face and $t = 0$ to the infinite point of the free surface).

If the solution of (4.25) is found, the mapping function $\zeta(w)$ can be determined in terms of function f by expression (4.18) and the complex velocity at any point of the flow region by formula (4.14).

The free surface of a fluid is determined in terms of $f(t)$ by the following parametric equations obtained from the formula (4.18):

$$\left.\begin{matrix}\xi(t)\\ \eta(t)\end{matrix}\right\} = \left\{\begin{matrix}\xi_B+\\ \eta_B-\end{matrix}\right\} c\int_t^1 t^{-\frac{3}{2}}(1-t)^{-\frac{1}{2}+\alpha}\exp\left[-t\int_0^1 \frac{f(\tau)}{\tau(\tau-t)}\,d\tau\right]\left\{\begin{matrix}\cos\\ \sin\end{matrix}\right\}[\pi f(t)]\,dt, \quad (4.27)\ (4.28)$$

where the constants c and η_B have the form

$$c = \left\{\cos\alpha_0\int_{\frac{1}{2}}^1 r^{-\frac{3}{2}}(1-r)^{-\frac{1}{2}+\alpha}(2r-1)^{-\alpha}\exp\left[-\int_0^1 \frac{f(\tau)\,d\tau}{\tau[\tau\{2-(1/r)\}-1]}\right]dr\right.$$
$$\left.-\int_0^1 t^{-\frac{3}{2}}(1-t)^{-\frac{1}{2}+\alpha}\exp\left[-t\int_0^1 \frac{f(\tau)}{\tau(\tau-t)}\,d\tau\right]\sin[\pi f(t)]\,dt\right\}^{-1}; \quad (4.29)$$

$$\eta_B = c\int_0^1 t^{-\frac{3}{2}}(1-t)^{-\frac{1}{2}+\alpha}\exp\left[-t\int_0^1 \frac{f(\tau)}{\tau(\tau-t)}\,d\tau\right]\sin[\pi f(t)]\,dt. \quad (4.30)$$

It should be noted that the asymptotic behaviour of the free surface at infinity can be obtained from equations (4.27), (4.28). Really, the analysis of (4.25) near the point $t = 0$ shows that $f(t) = O(t^{\frac{3}{2}})$ when $t \to 0$. This estimate together with (4.27), (4.28) considered at $t \to 0$, gives an asymptotic of function $\eta(\xi)$ at $\xi \to \infty$ which, as in the linearized theory of a thin wedge (Mackie 1962), has the form

$$\eta = K_1\xi^{-2}, \quad (4.31)$$

where $K_1 = K_1(\alpha)$.

The pressure distribution on the wedge face can be obtained from the Cauchy–Lagrange integral

$$2\,\mathrm{Re}\,[V(r) - \zeta(r)\,V'(\zeta)|_{\zeta=\zeta(r)}] + [V'(\zeta)\,\overline{V'(\zeta)}]_{\zeta=\zeta(r)} + p(r) = 0 \quad (\tfrac{1}{2} \leqslant r \leqslant 1), \quad (4.32)$$

where $p(r) = \Delta p/(\frac{1}{2}\rho v_0^2)$ is the dimensionless pressure on the wedge face,

$$\Delta p = p - p_0$$

(p_0 is the pressure on the free surface); point $r = \frac{1}{2}$ corresponding to the wedge apex $\zeta_A = -i$ and $r = 1$ to the point of contact ζ_B. Correspondence between the points of segment $[\frac{1}{2} \leqslant r \leqslant 1]$ and the co-ordinates ξ, η on the wetted wedge face is given by formula

$$\zeta(r) = \xi(r) + i\eta(r) = [\xi_B - c\sin\alpha_0 H_0(r)] + i[\eta_B - c\cos\alpha_0 H_0(r)], \quad (4.33)$$

where

$$H_0(r) = \int_r^1 r^{-\frac{3}{2}}(1-r)^{-\frac{1}{2}+\alpha}(2r-1)^{-\alpha}\exp\left[-\int_0^1 \frac{f(\tau)}{\tau[\tau\{2-(1/r)\}-1]}d\tau\right]dr. \quad (4.34)$$

Functions $[V'(\zeta)\,\overline{V'(\zeta)}]_{\zeta=\zeta(r)}$, $\mathrm{Re}\,[\zeta(r)\,V'(\zeta)|_{\zeta=\zeta(r)}]$

and $\mathrm{Re}\,V(r)$ in (4.32) have the form

$$[V'(\zeta)\,\overline{V'(\zeta)}]_{\zeta=\zeta(r)} = \left[\xi_B - \frac{c_0^2}{c}\sin\alpha_0 G_0(r)\right]^2 + \left[-\eta_B + \frac{c_0^2}{c}\cos\alpha_0 G_0(r)\right]^2, \quad (4.35)$$

where

$$G_0(r) = \int_r^1 (1-r)^{-1-\alpha}(2r-1)^{-1+\alpha}\exp\left[\int_0^1 \frac{f(\tau)}{\tau[\tau\{2-(1/r)\}-1]}d\tau\right]dr; \quad (4.36)$$

$$\mathrm{Re}\,[\zeta(r)\,V'(\zeta)|_{\zeta=\zeta(r)}] = [\xi_B - c\sin\alpha_0 H_0(r)]\,[\xi_B - (c_0^2/c)\sin\alpha_0 G_0(r)] - [\eta_B - c\cos\alpha_0 H_0(r)]\,[-\eta_B + (c_0^2/c)\cos\alpha_0 G_0(r)]; \quad (4.37)$$

$$\mathrm{Re}\,V(r) = \tfrac{1}{2}(\xi_B^2+\eta_B^2) + \int_r^1 r^{-\frac{3}{2}}(1-r)^{-\frac{1}{2}+\alpha}(2r-1)^{-\alpha} \times \exp\left[-\int_0^1 \frac{f(\tau)}{\tau[\tau\{2-(1/r)\}-1]}d\tau\right][c_0^2 G_0(r) - c(\xi_B\sin\alpha_0 + \eta_B\cos\alpha_0)]\,dr. \quad (4.38)$$

Given the above formulas for the pressure on the wedge face it is possible to estimate the behaviour of the pressure curve in the vicinity of the wedge apex. For this purpose it is sufficient to differentiate the Cauchy–Lagrange equation (4.32) with respect to r, to take into account the singularities at $r = \frac{1}{2}$ of the improper integrals $H_0(r)$ and $G_0(r)$ and to use formula (4.33) connecting variable r with the similarity variables ξ and η on the wedge. As a result we have

$$p = p_A - K_2\xi^{2\alpha/(1-\alpha)}, \quad (4.39)$$

where p_A is the pressure at the wedge apex and $K_2 = K_2(\alpha)$.

5. Method of numerical integration of the basic integral equation of the problem

For the numerical integration of (4.25) the method of successive iterations has been used. Below we dwell on some peculiarities of realization of this method for the given equation.

Point $t = 1$, as seen from the equation, is the singular point of the integrand of the outer integral $I(t)$. Integral $I(t)$ has to be convergent at this point since function $f(t)$ has to be bounded, by definition, on segment $[0, 1]$ including its ends. Let us analyze the behaviour of the integrand of integral $I(t)$ near the point $t = 1$.

We denote by β_0 the angle between the wedge face and free surface at the point of contact B. Then we have

$$f(1) = \tfrac{1}{2} + \alpha - \beta \quad \left(\beta = \frac{\beta_0}{\pi} \geqslant 0\right). \quad (5.1)$$

Now the Cauchy-type integral in (4.25) has the following representation near the point $t = 1$

$$\int_0^1 \frac{f(\tau)}{\tau(\tau-t)}\,d\tau = (\tfrac{1}{2}+\alpha-\beta)\ln(1-t)+\omega(t).$$

The following estimates for the functions standing under the integrals in (4.25) near the point $t = 1$ ($t < 1$) can be obtained

$$(1-t)^{-1-\alpha}\exp\left[t\int_0^1 \frac{f(\tau)}{\tau(\tau-t)}\,d\tau\right] = (1-t)^{-\frac{1}{2}-\beta}e^{\omega(t)},$$

$$t^{-\frac{3}{2}}(1-t)^{-\frac{1}{2}-\alpha}\exp\left[-t\int_0^1 \frac{f(\tau)}{\tau(\tau-t)}\,d\tau\right] = t^{-\frac{3}{2}}(1-t)^{-1+\beta}e^{-\omega(t)}.$$

Thus we find from (4.25) that $f'(t)$ behaves near $t = 1$ as $(1-t)^{-\frac{1}{2}-2\beta}$. Hence integral $I(t)$ at the point $t = 1$ is an ordinary improper integral which converges if and only if the following condition is satisfied:

$$\beta < \tfrac{1}{4}. \tag{5.2}$$

Thus, the magnitude β_0 of the angle between the free surface and the wedge face at the point of contact cannot exceed $\frac{1}{4}\pi$ for any wedge angle.

From conditions (5.1) and (5.2) it follows in turn that, if we use the iterations method, then for existence of every successive iteration f_{n+1} it is necessary that all the previous iterations would satisfy the condition

$$\tfrac{1}{4}+\alpha < f_k(1) < \tfrac{1}{2}+\alpha \quad (k=0, 1, \ldots, n) \tag{5.3}$$

which is the condition of convergence of integral $I(t)$ at the point $t = 1$.

It can be shown that condition (5.3) gives a possibility of constructing as many iterations as desired. Therefore, let us take as zero approximation a one-parameter family Ω of suitable (monotone, vanishing at $t = 0$ and providing convergence of $I(t)$ at $t = 0$) curves $f_0(t)$ ($0 \leqslant t \leqslant 1$) with parameter $F_0 \equiv f_0(1)$ belonging to segment $R = [\frac{1}{4}+\alpha, \frac{1}{2}+\alpha]$. Substituting into (4.25) the function $f_0(t) \in \Omega$ with $F_0 = \frac{1}{2}+\alpha$ we obtain that $F_1 \equiv f_1(1) = 0$. If $F_0 = \frac{1}{4}+\alpha$, it follows from (4.25) that $F_1 = \infty$. Thus, choosing as zero approximations the curves with $F_0 \in R$, we obtain the first iterations with $0 \leqslant F_1 < \infty$, and then there necessarily exists a smaller segment $R^{(1)}$ (lying entirely in R) such that the values $F_0 \in R^{(1)}$ will correspond to $F_1 \in R$ and $0 \leqslant F_2 < \infty$. Carrying out the same reasoning for the family of functions $f_1(t)$ with $F_1 \in R$ and then continuing this process further, we can obtain an unlimited sequence of segments $R^{(n)}$ contained in each other such that, at $F_0 \in R^{(n)}$, the above process makes it possible to construct at least $(n+1)$ iterations; however, the following iterations, beginning with a certain number, will not in general exist; in fact, it is sufficient that F_{n+1} should be outside the segment R and under this condition the $(n+2)$-th iteration would not exist.

The sequence of continuously decreasing segments $R^{(n)}$, when $n \to \infty$, determines (at least) one point F_0^*, by approaching which we can obtain as many iterations of (4.25) as desired.

It is clear from the above that with this method of constructing the successive iterations the process of iterations for (4.25) will not converge in the usual sense and can prove to be only asymptotically convergent. The asymptotic convergence in this case is understood in the following sense: the number of 'convergent' iterations of a given equation can be as great as desired but the following iterations generally speaking, do not exist.

For the numerical integration of (4.25) we have taken as zero approximation $f_0(t)$ $(0 \leqslant t \leqslant 1)$ the family of monotone increasing functions having, near the ends of the integration interval, the following representation (arising from the elementary analysis of (4.25))

$$f(t) = O(t^{\frac{3}{2}}) \quad \text{when} \quad t \to 0, \tag{5.4}$$

$$f(t) = F_0 - \gamma(1-t)^{\frac{1}{2}-2\beta} \quad \text{when} \quad t \to 1 \quad (0 < \beta < \tfrac{1}{4}). \tag{5.5}$$

The value $F_0 = f_0(1)$ has been taken as free parameter.

All the integrals in (4.25) have been computed with the variable step of integration decreasing near $t = 1$, the number of steps having been chosen in such a way that the distance between the last point of integration and 1 is equal to some small value ϵ which choice was determined by the necessary accuracy of calculation. The computation has shown that the value ϵ is of the order of 10^{-12}–10^{-18} (depending on the value of α) decreasing with decreasing α. The refinement of the step of integration to such a small magnitude is due to the very special behaviour of the integrands of (4.25) near $t = 1$. The partial sums of the integrals near the ends $t = 0$ and $t = 1$ have been computed with the help of obtained estimations of the corresponding integrands near these points.

As would be expected, the process of iterations for (4.25) has proved to be asymptotically convergent. The computation has shown that for obtaining the solution $f(t)$ to the practically required precision it is sufficient to construct only 10–12 iterations, 4–5 mean iterations having proved to be almost coinciding.

The computation has confirmed to high accuracy the character of behaviour of the function $f(t)$ near $t = 1$, described by formula (5.5). However, the curve $f(t)$ can be represented in the form of (5.5) only in the extremely small neighbourhood of point $t = 1$. Such behaviour of $f(t)$ has required the above mentioned refinement of the step of integration near $t = 1$.

6. Numerical results of solving the wedge entry problem

The numerical computations have been done for the complete wedge angles $2\alpha_0 = 0{\cdot}036°$, $0{\cdot}36°$, $3{\cdot}6°$, $6°$, $18°$, $60°$ and $120°$ ($\alpha = 0{\cdot}0001$, $0{\cdot}001$, $0{\cdot}01$, $\frac{1}{60}$, $0{\cdot}05$, $\frac{1}{6}$, $\frac{1}{3}$).

The curves $f(t)$, which are the solution of (4.25) for angles $\alpha = \frac{1}{20}$, $\frac{1}{6}$ and $\frac{1}{3}$, are presented in figure 8. All these curves have very small ordinates at the large interval adjoining zero and sharply increase immediately near the point $t = 1$ (the last points of the curves at $t = 1$ are denoted in figure 8 by heavy points). The curves $f(t)$ for $\alpha < \frac{1}{20}$ practically coincide in the figure with the axis of abscissas and the straight line parallel to the axis of ordinates and passing through the point $t = 1$.

With the help of obtained functions $f(t)$ the free surface curves have been computed from the formulae (4.27)–(4.30). For the total wedge angles $2 \times 3°$, $2 \times 9°$, and $2 \times 30°$ these curves are presented in figure 9. It is seen here that with increased wedge angle the free-surface disturbance, as would be expected, increases and the splash adjoining the wedge increases lengthwise getting at the

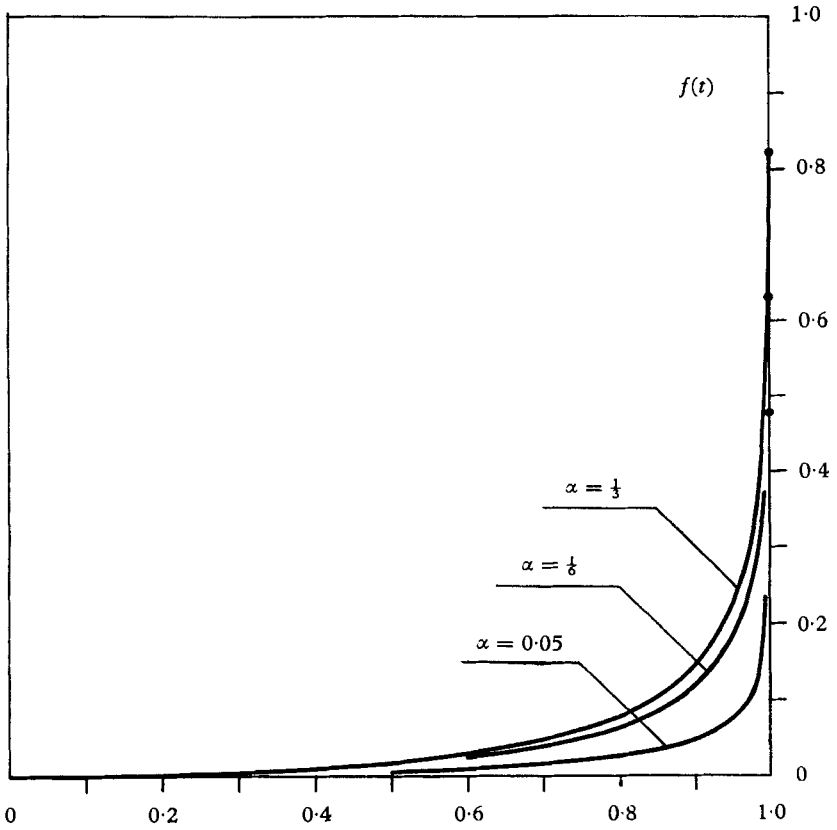

FIGURE 8. Curves $f(t)$ for $\alpha = 0{\cdot}05$, $\frac{1}{6}$ and $\frac{1}{3}$.

same time thinner and thinner by its apex. With decreased angle α the maximum height of the splash and the region of the free surface disturbance decrease. The curve $\eta_B = \eta_B(\alpha)$ of the maximum splash heights *versus* α is presented in figure 10. Numerical values of magnitude η_B for different angles α are presented together with some other data of numerical computations in table 1. Figure 11 gives the dependence $\eta_B/(\pi\alpha)$ on $\log\alpha$. From the analysis of this dependence we may conclude that with $\alpha \to 0{\cdot}5$ the height η_B seems to increase only up to some limit value close to $\eta_B \approx 3$.

It is customary to assume that the linearized theory gives in general an infinite splash height. However, Mackie (1962) has obtained from the linearized theory on the basis of reasonable concepts the following approximate formula for the splash height

$$\frac{\eta_B}{\pi\alpha} = \frac{2}{\pi}\ln\frac{1}{\pi\alpha}. \tag{6.1}$$

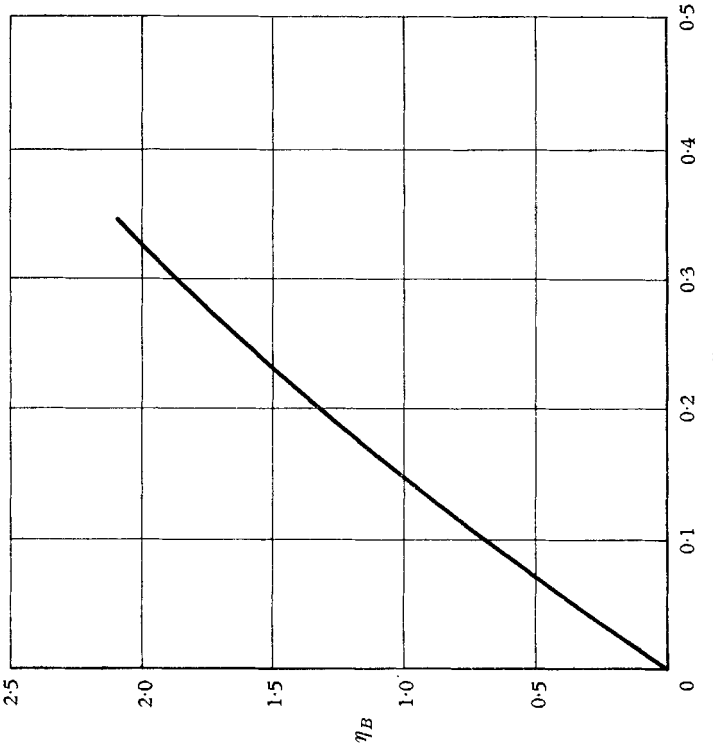

FIGURE 10. The maximum height of the splash η_B *versus* α.

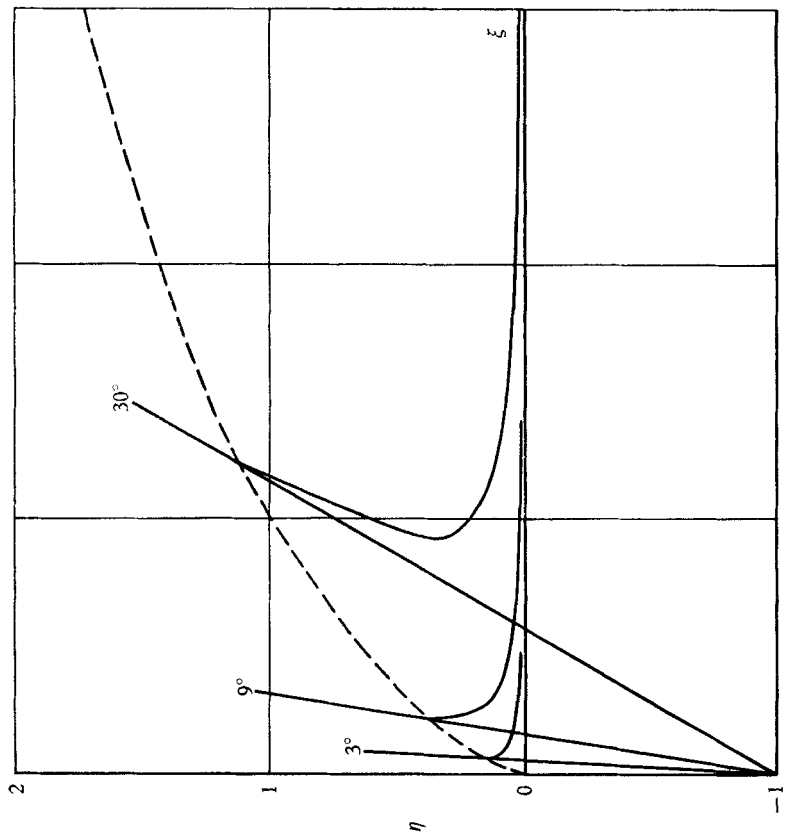

FIGURE 9. The free surfaces $\eta = \eta(\xi)$ for $\alpha_0 = 3°$, 9° and 30°.

Careful treatment of our numerical data gives for the small angles the asymptotic dependence

$$\frac{\eta_B}{\pi\alpha} = A \ln\frac{1}{\pi\alpha} + B, \tag{6.2}$$

the constant A practically being equal to $2/\pi \approx 0{\cdot}637$ and $B \approx 0{\cdot}82$. It is seen from here, that Mackie's formula, theoretically rightly describing the dependence $\eta_B/(\pi\alpha)$ on α when $\alpha \to 0$, gives a small relative error for the splash height η_B only for the extraordinary small wedge angles.

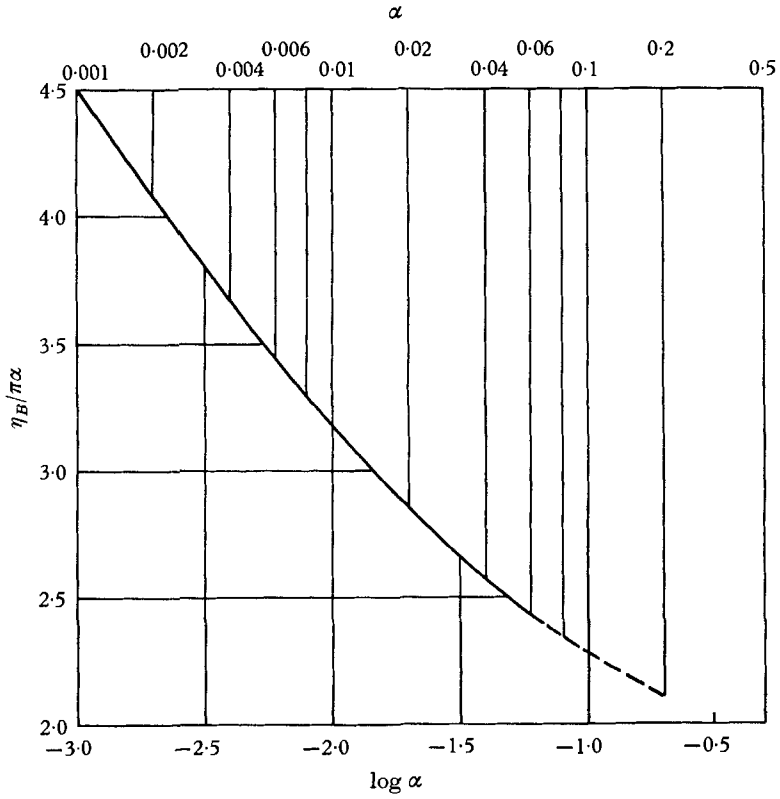

FIGURE 11. The curve $\eta_B/(\pi\alpha)$ *versus* $\log\alpha$.

α	η_B	β	$K_1/(\frac{1}{3}\alpha)$	p_A	$\dfrac{P}{\mathrm{tg}^2\alpha_0}\Big/\left(\dfrac{P}{\mathrm{tg}^2\alpha_0}\right)_{\alpha_0\to 0}$
10^{-4}	0·0019	0·100	1·02	1·00	1·00
10^{-3}	0·014	0·100	1·03	1·00	1·01
10^{-2}	0·099	0·094	1·08	1·04	1·10
$\frac{1}{60}$	0·153	0·089	1·11	1·06	1·17
$\frac{1}{20}$	0·39	0·072	1·31	1·2	1·5
$\frac{1}{6}$	1·13	0·036	2·3	2·0	3·1
$\frac{1}{3}$	2·0	0·011	12	5	6

TABLE 1.

For comparing the obtained free surfaces with the data of linearized theory the free surface curves are presented in figure 12 in the form of the dependence $\eta/\mathrm{tg}\,(\pi\alpha)$ on ξ. The free-surface curve obtained from the linearized theory and described by the formula

$$\frac{\eta}{\pi\alpha} = \frac{1}{\pi}\left[\ln\left(1+\frac{1}{\xi^2}\right) + 2\xi\,\mathrm{arc\,tg}\frac{1}{\xi} - 2\right] \tag{6.3}$$

is represented on the same figure. Our numerical results, as it is seen from the figure, approach the latter when $\alpha \to 0$.

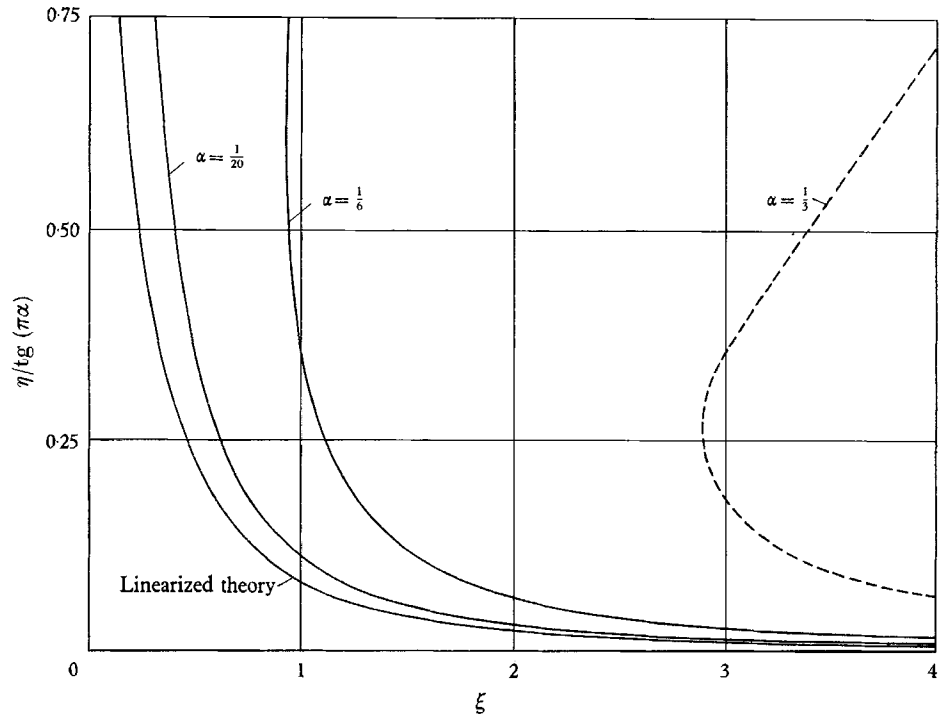

FIGURE 12. The curves $\eta/\mathrm{tg}\,(\pi\alpha)$ *versus* ξ for different α.

At infinity the free-surface curves behave according to (4.31) as $\eta \approx K_1(\alpha)\,\xi^{-2}$. The treatment of our numerical results shows that at sufficiently large ξ the equation of the free surface can be represented in the form

$$\frac{\eta}{\pi\alpha} = \frac{1}{3\pi\xi^2}[1+\epsilon_1(\alpha)] - \frac{0{\cdot}028}{\xi^3}[1-\epsilon_2(\alpha)], \tag{6.4}$$

where $\epsilon_1(\alpha)$ and $\epsilon_2(\alpha)$ are the functions vanishing when $\alpha \to 0$. So, it follows from the computations that, at small α, $K_1(\alpha) = \frac{1}{3}\alpha$ that coincides with the result of the linearized theory. Numerical values of the ratio $K_1/(\frac{1}{3}\alpha)$ are presented in table 1.

The free-surface behaviour near the point of contact with the wedge can be characterized by the value $\beta = \beta_0/\pi$, where β_0 is the angle between the free surface and the wedge at the point of contact. The values β for the different wedge angles

have been computed with the help of corresponding values $f(1)$ from the formula (5.1). The curve $\beta = \beta(\alpha)$ is represented in figure 13 (numerical data are given in table 1). At small α this relationship can be expressed to high accuracy by the formula $\beta = 0{\cdot}1 - \frac{2}{3}\alpha$.

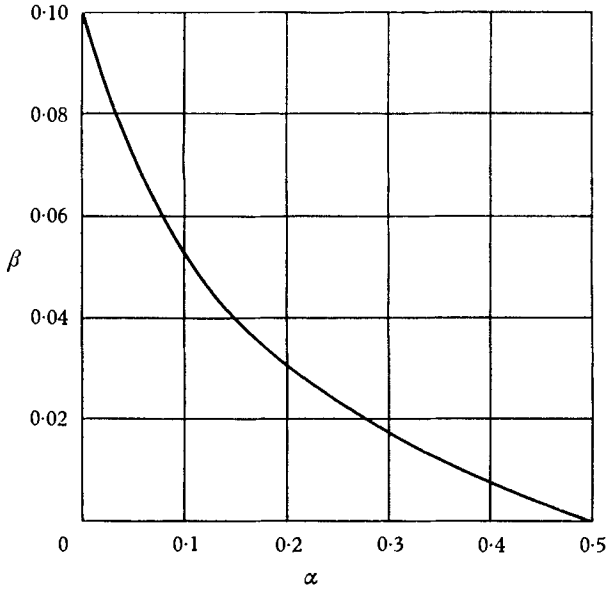

FIGURE 13. The curve of the angle of contact β *versus* α.

It is seen from the dependence $\beta = \beta(\alpha)$ that the angle of contact of free surface with the wedge increases with decreased wedge angle. However, with $\alpha \to 0$ the angle β_0 does not practically exceed 18°. On the other hand, if $\alpha = 0$ then from the statement of the problem it follows directly that $f(t) \equiv 0$ and $\beta_0 = \frac{1}{2}\pi$. Thus, the free surface inclination to the wedge face at the point of contact has a discontinuity at $\alpha = 0$ as a function of α. This is similar to the problem of symmetrical impact of a water wedge on a solid wall. Really, Cumberbatch's (1960) approximate computations have shown that with the decrease of half-angle of a fluid wedge from 22·5° to 11·25° the tip angle of the stream on a wall increased from 3° to 4·8°. Therefore, it is reasonable to suppose that with the fluid wedge angle tending to zero the tip angle of the stream would approach some finite value rather than zero.

The dependence $\eta_B = \eta_B(\alpha)$ for the wedge entry (see figure 10) shows that with $\alpha \to 0$ the maximum splash η_B tends to zero, and the region of disturbance vanishes, i.e. the picture of flow in the case of a wedge entry remains in the large continuous when $\alpha \to 0$ and at $\alpha = 0$.

The discontinuity of function $\beta = \beta(\alpha)$ at $\alpha = 0$ is the consequence of the model of ideal liquid and the similar result in the hydrodynamics of an ideal liquid is not a single one. So, in the flow past the plate inclined to the flow direction at angle α, the fluid velocity at the edges of the plate is infinite at any $\alpha \neq 0$, although

at $\alpha = 0$ the fluid velocity at the edges is equal to the velocity at infinity. But the picture of flow past the plate, as in the case of a wedge entry, changes on the whole, continuously when $\alpha \to 0$ and at $\alpha = 0$.

For estimating the accuracy of obtained numerical results we have checked two conditions: the incompressibility of a fluid and the conservation of the arc length along the free surface.†

In order to verify the incompressibility condition we have computed the area S of the flow region above the axis of abscissas and then this area was compared with the area Δ of that part of the wedge which was under the axis of abscissas. For verifying the second condition mentioned above we have computed the length l of the part of the free surface from the point of contact B to that point of the free surface which ordinate could be practically taken as zero, and then the value l was compared with the abscissa ξ^* of this point.

For the wedge angles $2\alpha_0$ up to 18° ($\alpha = 0{\cdot}05$) inclusive, the condition of conservation of the arc length ($\xi^* - l = 0$) has proved to be satisfied to within $|(\xi^* - l) : \eta_B| = 0{\cdot}004$ and the incompressibility condition to within

$$|S/\Delta - 1| = 0{\cdot}01.$$

When $2\alpha_0 > 18°$ the computations have been done with a smaller accuracy. So, for $\alpha = \frac{1}{6}$ the computations have been done to within 0·01 and 0·03, respectively, and for $\alpha = \frac{1}{3}$ (the wedge angle $2\alpha_0 = 120°$) only an approximate estimation has been obtained (therefore the curves for $\alpha_0 = 60°$ are drawn in the figures by dotted lines). Increase of the accuracy of numerical results and their extension onto the angles $2\alpha_0 > 120°$ do not induce great difficulties and demand only more machine time.

By means of obtained curves $f(t)$ for different α the distribution of hydrodynamic pressure on the wedge face has been computed from the formulas (4.32)–(4.38). As would be expected, the computations have shown that the pressures on the wedge decreased with the decrease of the wedge angle. The dimensionless pressure $p = \Delta p/(\frac{1}{2}\rho v_0^2)$ at the wedge apex tends with $\alpha \to 0$ to a value close to 1, and the pressures on the wedge face tend to zero. The value $p_A = 1$ can be obtained also from indirect theoretical considerations. For this purpose it is sufficient to use the estimate (4.39) for the behaviour of the pressure in the neighbourhood of the wedge apex and to substitute there the values of pressure at any two points, calculated by the linearized theory (according to the linearized theory the pressure at the wedge apex itself is infinite). Numerical values of the dimensionless pressure p_A at the wedge apex are presented for different α in table 1.

As the pressures on the wedge for the small angles α are very small (everywhere except the neighbourhood of the apex), it is more convenient to compare the pressure distribution curves for different wedge angles by considering the dependence of $p/\mathrm{tg}\,\alpha_0$ on η rather than p on η. Figure 14 presents the relations

† As has been shown by Wagner (1932), the distance (measured along free surface) between two arbitrary fluid particles on the free surface remains constant in the similarity flow under consideration.

$p/\mathrm{tg}\,\alpha_0$ *versus* η for different α ($\eta = -1$ is the wedge apex). The pressure curve for $\alpha = 0{\cdot}0001$ practically coincides with the curve given by the linearized theory:

$$\frac{p}{\alpha_0} = \frac{1}{\pi}\ln\frac{1-\eta}{1+\eta}. \tag{6.5}$$

For $\alpha_0 > 3°$ the pressure distribution curves, as seen from the graphs, begin quickly to deviate from the pressure curve of the linearized theory and for α_0 close to 30° these curves have nothing in common with the results of the linearized

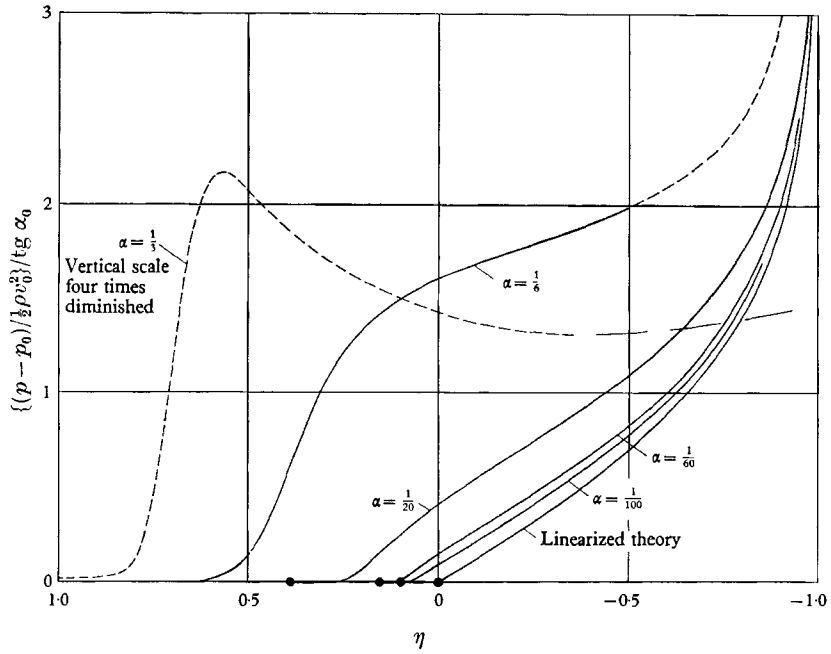

FIGURE 14. The curves of the distribution of the dimensionless pressure p divided by $\mathrm{tg}\,\alpha_0$ along the wedge face for different angles α.

theory. The ordinates $p/\mathrm{tg}\,\alpha_0$ near the wedge apex ($\eta = -1$) become for the small α, as would be expected, very large (but finite), and therefore the values $p/\mathrm{tg}\,\alpha_0$ at $\eta = -1$ are not included in the figure. As seen from figure 14 the pressure at the upper part of the splash proves to be practically equal to zero (the ends of the splash jets are denoted on the figure by heavy points).

The pressure distribution curve for $\alpha_0 = 60°$ shows that for the large angles α_0 the maximum of the pressure displaces from the wedge apex to some point on the face of the wedge, this point being situated for the large α_0 above the level of the initially undisturbed free surface. This qualitative result coincides with the Borg (1959) approximate computations.

With the help of obtained pressure curves we have computed the value of the dimensionless total drag force

$$P = 2\int_0^{\xi_B} \frac{\Delta p}{\frac{1}{2}\rho v_0^2}\,d\xi$$

acting on the entering wedge (both its faces). The actual drag force P^* is connected with the value P by the obvious relation: $P^* = \rho v_0^3 t P$. The dependence $P/\mathrm{tg}^2\,\alpha_0$

on α is represented in figure 15. Numerical values of the ratio of $(P/\mathrm{tg}^2\alpha_0)$ to the magnitude $(P/\mathrm{tg}^2\alpha_0)_{\alpha_0\to 0}$ obtained as the limit when $\alpha_0 \to 0$, are presented in table 1. The analysis of obtained data makes it possible to represent the force P for small wedge angles ($\alpha < 0,1$) in the form

$$P = 1{\cdot}765\,\mathrm{tg}^2\alpha_0 + 5{\cdot}8\,\mathrm{tg}^3\alpha_0, \tag{6.6}$$

where 1·765 is the magnitude given by the linearized theory.

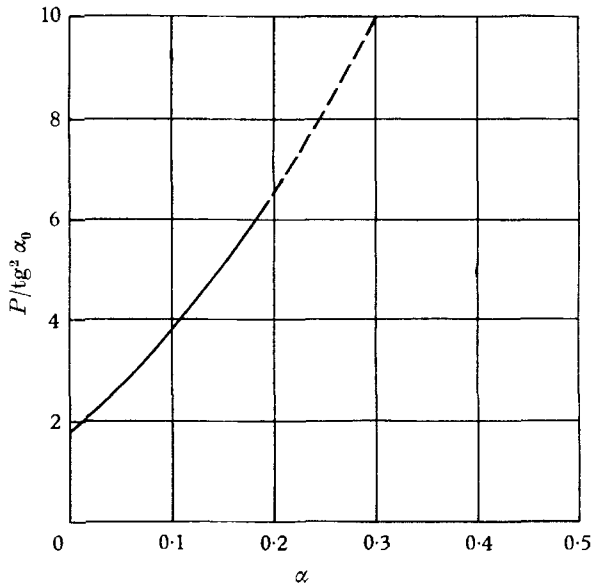

FIGURE 15. The dimensionless drag force P (divided by $\mathrm{tg}^2\alpha_0$) acting onto the entering wedge, *versus* α.

The presented results of numerical calculations for the wedge-water entry problem demonstrate the efficiency and practical applicability of the general method when using modern digitial computers.

The theoretical part of this work has been done at the former Institute of Mechanics of the USSR Academy of Sciences, in the Department of Prof. L. A. Galin, member of the Academy, to whom the author is grateful for many useful discussions. The development of the numerical methods of solving the wedge problem and all the calculations have been carried out by the author at the Computing Centre of the Academy.

The author is greatly indebted to Prof. G. K. Mikhailov for his constant attention to this work and many valuable ideas.

REFERENCES

BORG, S. F. 1957 Some contributions to the wedge-water entry problem. *Proc. Am. Soc. Civil Engrs, J. Engng Mech. Div.* **83**, no. EM2, Pap. 1214.

BORG, S. F. 1959 The maximum pressures and total force on straight-sided wedges with small dead-rise. *J. Am. Soc. Naval Engrs*, **71**, 559–561.

CUMBERBATCH, E. 1960 The impact of a water wedge on a wall. *J. Fluid Mech.* **7**, 353–374.

DOBROVOL'SKAYA, Z. N. 1965 Some non-linear problems of the similarity flow of incompressible fluid with free surface (in Russian). In: *Applications of the Theory of Functions in Continuum Mechanics*, vol. 2, pp. 150–170. Moscow.

DOBROVOL'SKAYA, Z. N. 1966 Numerical solution of integral equation of a two-dimensional problem of the similarity flow with free surface (in Russian). *J. Comput. Math. and Math. Phys.* **6**, 934–941.

GARABEDIAN, P. R. 1953 Oblique water entry of a wedge. *Comm. Pure and Appl. Math.* **6**, 157–165.

GRIGORYAN, S. S. 1956 Some problems of the hydrodynamics of slender bodies (in Russian). Thesis, Moscow Univ.

MACKIE, A. G. 1962 A linearized theory of the water entry problem. *Quart. J. Mech. and Appl. Math.* **15**, 137–151.

MOISEEV, N. N., BORISOVA, E. P. & KORIAVOV, P. P. 1959 Plane and axially symmetrical automodel (similarity) problems of stream impact. *Appl. Math. and Mech.* (PMM) **23**, 490–507.

PIERSON, J. D. 1950 The penetration of a fluid surface by a wedge. *Stevens Inst. Technol., Expt. Towing Tank Rep.* no. 387.

SAGOMONYAN, A. Y. 1956 Wedge entry into a compressible fluid (in Russian). *Vestnik Moscow Univ.* no. 2, 13–18.

WAGNER, H. 1932 Über Stoss- und Gleitvorgänge an der Oberfläche von Flüssigkeiten. *Z. angew. Math. und Mech.* **12**, 193–215.

INDEX

REVIEWS